Scientific
Research
Publishing

Synthesis of SiO$_X$ Nano-Powders Using a Microwave Plasma Torch at Atmospheric Pressure

Dong Hun Shin[1], Yun Seok Choi[2], Dong Jin Ku[2], Yong Cheol Hong[1*], Bong Ju Lee[2*]

[1]Plasma Technology Research Center, National Fusion Research Institute, Gunsan, Korea
[2]Department of Advanced Green Energy Environment, Handong Global University,
Pohang, Korea
Email: *ychong@nfri.re.kr, *bjlee@handong.edu

Abstract

The silicon oxide nano-powders (SiO$_x$-NPs) were obtained in an atmospheric microwave plasma torch using a gas-phase silicon tetrachloride (SiCl$_4$) with N$_2$ and H$_2$. The gas-phase SiCl$_4$ was injected with H$_2$ gas into the microwave plasma torch generated by N$_2$ and air swirl gas, and then the dark brown powders were deposited on the inner wall of a quartz tube. The sample was analyzed by an X-ray photoelectron spectroscopy (XPS), a scanning electron microscope (SEM), an energy dispersive spectrometer (EDS), and an X-ray diffraction (XRD). The average size and oxidation x values of synthesized SiO$_x$-NPs were approximately 230 nm and 0.91, respectively. Furthermore, the volumetric charge capacity is 1127 mAh/g and has 89.2% retention after 100 cycles.

Keywords

1. Introduction

Nanostructures have attracted considerable attention in many research fields due to their unique low-dimensional quantum size effects, interesting geometry, and potential applications in nanotechnology. Silicon oxide nano-powders (SiO$_x$-NPs) in particular have generated a great deal of interest for their outstanding semiconducting, mechanical, and optical properties, all of which enable them to be used as coating materials, sensitive sensors,

---

*Corresponding authors.

protective layers, and blue-light-emitting diodes. These future applications, however, impose more challenging standards for a range of cell perspectives, including energy density, power performance, cycle life, and safety. While issues in these parameters need to be addressed in parallel, the simultaneous improvement of the energy density and cycle life is more critical [1]-[3]. Of late, there has been a focus on SiO_x-NPs ($x \approx 1$) due its high charge/discharge efficiency and capacity as an alternative material to carbonaceous materials among secondary cell anode materials [4]-[7]. SiO_x-NPs are usually synthesized using chemical reaction routes which are often complex and offer a relatively small production yield [8] [9]. The adsorptive capabilities of nano-scaled SiO_x will exceed those of conventional SiO_x. In this context, we report a simple synthetic method of preparing SiO_x-NPs, making use of an atmospheric microwave plasma torch.

2. Experiment

Figure 1 shows the experimental setup for the preparation of SiO_x-NPs with the microwave plasma torch. The design and operation of the atmospheric microwave plasma torch are briefly summarized here for completeness, although they have been reported in detail in our previous literatures [10]-[13]. As shown in **Figure 1**, the microwave energy is supplied to the flowing gas at atmospheric pressure by a microwave generator, and efficient power transfer is achieved through a matching network, which basically consists of an auto-matcher, a matcher controller, and an isolator, namely, the microwave radiation generated from the magnetron passes through the circulator and the auto-matcher, is guided through a tapered waveguide, and enters the discharge tube made of a fused quartz. The center axis of the quartz dielectric tube, with an outer diameter of approximately 30 mm and a thickness of 2 mm, is located one-quarter wavelength from the short end of the waveguide and is perpendicular to the wide waveguide walls. The electric field induced by the microwave radiation in the quartz tube can be maximized by adjusting the auto-matcher. Additionally, the reflected power adjusted with the auto-matcher is less than 1% of the forward power. This produces a plasma torch with a high temperature and a high plasma density. The microwave plasma torch provides a highly unusual and reactive chemical environment at high temperatures. For example, the air microwave plasma torch produces plasma with a high temperature of ~6000 K and a high plasma density of ~10^{13}/cm^3 [14].

All the gas flows in **Figure 1** were controlled by mass flow controllers (MFCs). The silicon source in our experiment was silicon tetrachloride ($SiCl_4$), which has a high vapor pressure, low activation energy, and low cost.
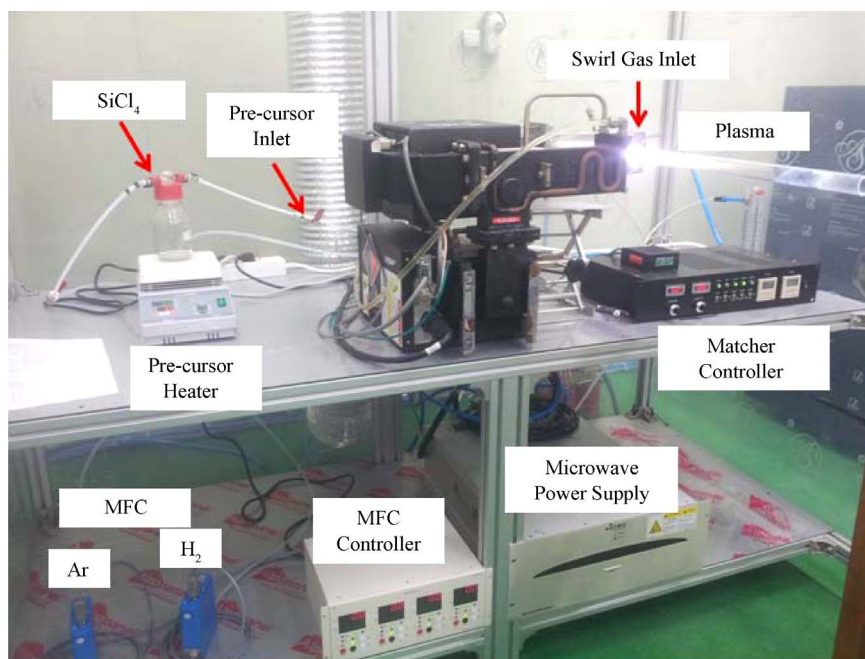

Figure 1. The presentation of the synthetic system of SiO_x-NPs with the atmospheric microwave plasma torch.

The properties mentioned above may be suitable for a plasma-enhanced gas-phase synthesis method at atmospheric pressure. $SiCl_4$ is handled in a glove box with a non-moisture atmosphere, and a bottle for $SiCl_4$ bubbling has to be packed well because of a moisture-sensitive reagent. $SiCl_4$ (99.9%, Aldrich) in the liquid solution is directly bubbled by argon gas and is axially injected with hydrogen gas through the Teflon tube, as shown in **Figure 1**, which guides a mixture of bubbled $SiCl_4$ and hydrogen gas into the center of the plasma flame. As shown in **Figure 1**, $SiCl_4$ in liquid solution and the inlet line of axial gases were maintained at about 65°C by making use of automatic-controlled heaters. Nitrogen and air as swirl gas enter the microwave plasma torch via four small holes in the tangential direction of the inner surface of the quartz tube, not shown in **Figure 1**, and hydrogen as an additive gas was used for partial oxidation of silicon oxide formed from the decomposition and reduction of $SiCl_4$. The SiO_x-NPs were synthesized by 20 lpm of N_2 and 0.5 lpm air as swirl gases and 10 lpm of N_2 gas with 10 lpm of H_2 gas for $SiCl_4$ carrier and then $SiCl_4$ liquid pre-cursor of approximately 1 ml per minute (ml/min) were injected into the microwave plasma torch operated at 2 kW power. Furthermore, the swirl gases of N_2 were injected before sampling to cool down because as-produced SiO_x-NPs had avoided oxidation under high temperature conditions. Once the synthesis of SiO_x-NPs starts by passing through the plasma flame, a red-brownish light, like a flash, emits from the torch flame, not shown in this paper. All the samples were taken from deposits inside the quartz tube.

3. Results and Discussion

Figure 2 depicts the graph of the size distribution bars with an inert scanning electron micro-scope (SEM) image, and energy dispersive spectrometer (EDS) spectra of synthesized SiO_x-NPs. The photo image of **Figure 2(a)** is the synthesized SiO_x-NPs by the microwave plasma torch. Kim *et al.* reported different colors of SiO_x powders in terms of oxide x values. The SiO_x sample colors were strongly dependent on their valence states and became brighter when x increased. When the x value was 1.18, the color was brown, whereas it was almost white at an x value of 1.83 [15]. Additionally, the size distribution of synthesized SiO_x-NPs was analyzed using an SEM image (insert image) and the average size was approximately 230 nm, as shown in **Figure 2(b)**. **Figure 2(c)** illustrates the EDS analysis data in the form of spectra, where the peaks corresponding to the elements Si, O, and carbon appear to be dominant, as seen in the spectra, and the data listed in **Table 1** show a small amount of carbon. It is believed that the trace of carbon in the spectrum was detected due to the atmospheric pressure synthesis process and during the sampling of SiO_x-NPs. For this reason, the carbon spectra were detected by EDS analysis. Hence, the synthesized SiO_x-NPs were examined by performing an EDS analysis. To determine the valence state of the Si in the SiO_x in synthesized SiO_x, an X-ray Photoelectron Spectroscopy (XPS) analysis was conducted.

Figure 3(a) shows the Si-2p binging energy spectra of Si in the SiO_x from the X-ray photoelectron spectroscopy (XPS). The analysis condition of XPS (AXIS Ultra DLD, Kratos Inc.) was a monochromatic Al Kα (1486.6 eV, 150W). The measured band of the Si-2p binding energy was divided into five sub bands: Si (99.8 eV), $SiO_{0.5}$ (100.7 eV), $SiO_{1.0}$ (101.5 eV), $SiO_{1.5}$ (102.5 eV), and $SiO_{2.0}$ (103.5 eV). The x value was calculated using the following equation [16]:

$$x = \{(0.0 \times a) + (0.5 \times b) + (1.0 \times c) + (2.0 \times e)\} / (a + b + c + d + e)$$

where, x is the valence state of the Si in the SiO_x, and a, b, c, d, and e represent the intensity of the Si-2p binding of the Si, $SiO_{0.5}$, $SiO_{1.0}$, $SiO_{1.5}$, and $SiO_{2.0}$, respectively. The normalized intensities for calculating the x values are 0.53 of Si, 0.12 of $SiO_{0.5}$, 0.37 of $SiO_{1.0}$, 0.77 of $SiO_{1.5}$, and 0.32 of $SiO_{2.0}$, respectively. In this context, the x value of synthesized SiO_x was 0.91. Additionally, a comparison with the X-ray diffraction (XRD) pattern of synthesized SiO_x and commercial SiO_2 NPs are shown in **Figure 3(b)**. The commercial SiO_2 NPs were prepared

Table 1. Spectrum data from EDS analysis of synthesized SiO_x-NPs.

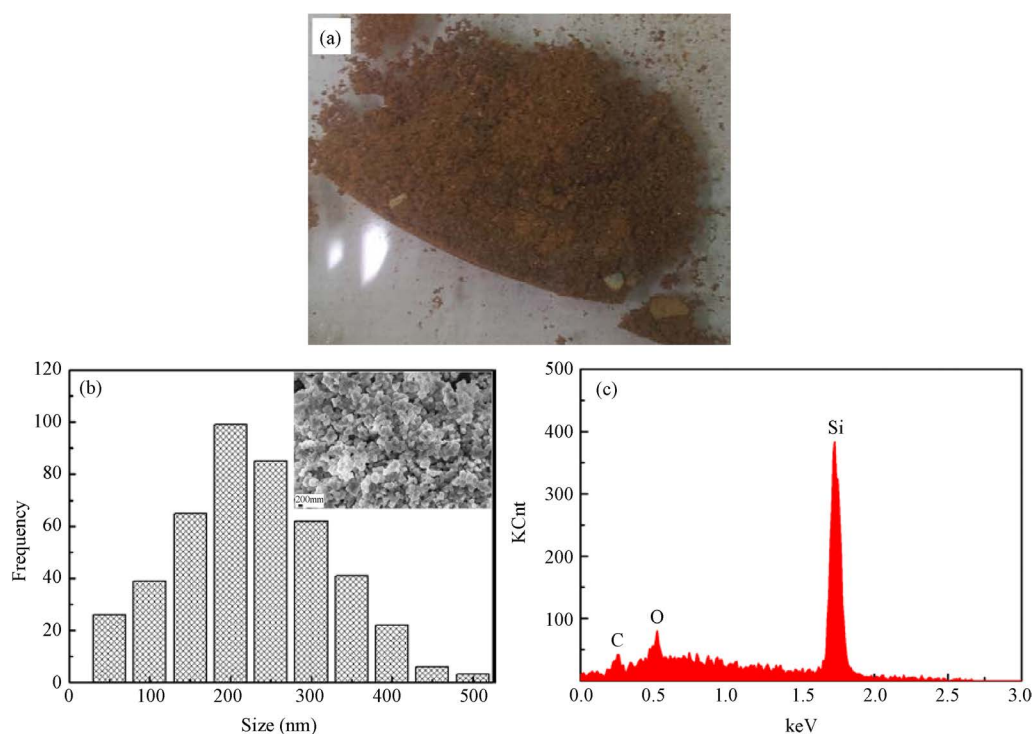| Elements	Wt%	At%
C	0.36	0.83
O	26.56	38.36
Si	73.08	60.81

Figure 2. (a) Photo, (b) size distribution bars with insert SEM image, and (c) spectra data from EDS of synthesized SiO_x-NPs.
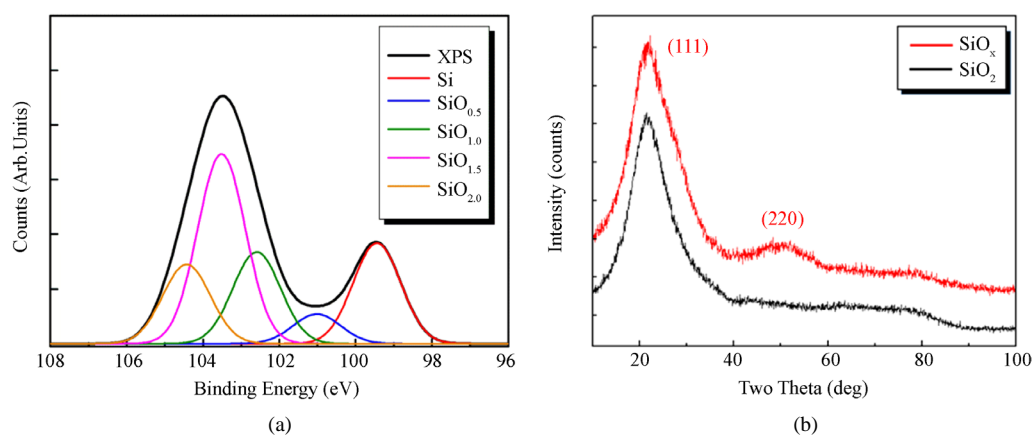

Figure 3. (a) The Si-2p binding energy spectra of synthesized SiO_x-NPs from XPS (the value indicates a valence state of Si in SiO_x) and (b) XRD spectra of synthesized SiO_x and Ref. SiO_2 NPs.

with over 99.5% of purity and 10 - 20 nm of average size from Sigma Aldrich (CAS No. 7631-86-9). The XRD pattern of synthesized SiO_x-NPs is shown in **Figure 3(b)**, red line, the Si (111, 220) diffraction peak. Further, Sun, W. *et al.*, the commercial SiO precursor, has only two broad humps centered at ~23 and ~51 degrees and was observed in the XRD pattern [17]. In this context, the characteristics of synthesized SiO_x-NPs which have a 0.91 x value are very close to the SiO.

Figure 4 shows the volumetric charge (delithiation) capacity of the anodes using the Ref. Si and synthesized SiO_x-NPs as a function of cycle number and Coulomb efficiency at a 0.2 C rate between 0.01 and 1.5 V in a coin-type half-cell. The Ref. Si-NPs (average size of approximately 200 nm) showed before and after 100 cycles of charge/discharge capacity at 2343 mAh/g and 511 mAh/g, respectively. The Ref. Si-NPs showed that the highest first charge/discharge capacity faded out quickly with the increase in the number of cycles. Therefore, the retention
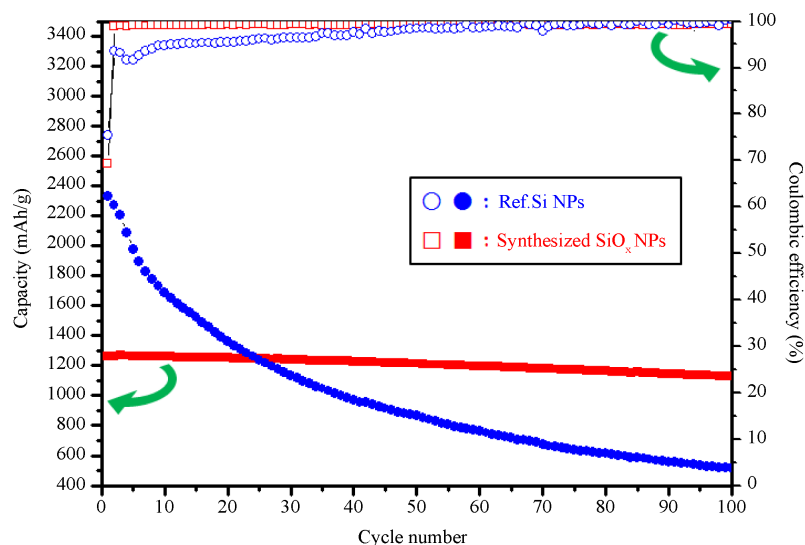
Figure 4. Cycle performances of the anodes using by the Ref. Si and synthesized SiO_x-NPs.

ratio of Ref. Si-NPs is only 21.8%. However, the synthesized SiO_x-NPs demonstrated very stable cycle performance. The synthesized SiO_x-NPs showed before and after 100 cycles charge/discharge capacity at 1264 mAh/g and 1127 mAh/g, respectively. Therefore, the retention rate is 89.2% after 100 charge/discharge cycles. These results were due to the large portion of Li-based oxides such as Li_2O and Li_4SiO_4 on the nano-particles. Li_2O and Li_4SiO_4 are inactive to an electrical field, but they can serve as a buffer to the expansion of Si during the lithiation process. These buffers can result in good cycle performance from the next cycle [15] [18] [19].

4. Conclusion

The microwave plasma torch method has been developed to synthesize SiO_x-NPs. The high-temperature microwave plasma flame evaporated the $SiCl_4$ pre-cursor and produced SiO_x-NPs through the cooling of Si atoms in the downstream direction of nitrogen and air plasma torch. The SiO_x-NPs can easily be obtained by making use of the microwave plasma torch, although the synthetic approach reported here is not finely controlled. The x value and average size of the synthesized SiO_x were 0.91 and approximately 230 nm, respectively. The volumetric charge capacity is 1127 mAh/g and 89.2% retention after 100 cycles. This method may be suitable for direct continuous preparation and mass production of SiO_x-NPs by adding a collection chamber, such as filtration apparatus. This work might provide the synthesis for controlling the x-value in SiO_x-NPs by oxygen content.

Acknowledgements

References

[1]   Moon, J.S., Alegaonkar, P.S., Han, J.H., Lee, T.Y. and Yoo, J.B. (2006) Enhanced Field Emission Properties of Thin-Multiwalled Carbon Nanotubes: Role of SiO_x Coating. *Journal of Applied Physics*, **100**, Article ID: 104303. http://dx.doi.org/10.1063/1.2384795

[2]   Hwang, T.H., Lee, Y.M., Kong, B., Seo, J. and Choi, J.W. (2012) Electrospun Core-Shell Fibers for Robust Silicon Nanoparticle-Based Lithium Ion Battery Anodes. *Nano Letters*, **12**, 802. http://dx.doi.org/10.1021/nl203817r

[3]   Wei, Q., Meng, G.W., An, X.H., Hao, Y.F. and Zhang, L.D. (2006) Synthesis and Photoluminescence of Aligned Straight Silica Nanowires on Silicon Substrate. *Solid State Communications*, **138**, 325-330. http://dx.doi.org/10.1016/j.ssc.2006.03.022

[4]   Jung, C.O. and Park, D.W. (2013) Synthesis of $SiO_{(x)}$ Powder Using DC Arc Plasma. *Journal of Nanoscience and*

Nanotechnology, **13**, 1153-1158. http://dx.doi.org/10.1166/jnn.2013.6035

[5] Seong, I.W. and Yoon, W.Y. (2010) Electrochemical Behavior of a Silicon Monoxide and Li-Powder Double Layer Anode Cell. *Journal of Power Sources*, **195**, 6143-6147. http://dx.doi.org/10.1016/j.jpowsour.2010.01.065

[6] Yang, J., Takeda, Y., Imanishi, N., Capiglia, C., Xie, J.Y. and Yamamoto, O. (2002) SiO_x-Based Anodes for Secondary Lithium Batteries. *Solid State Ionics*, **152-153**, 125-129. http://dx.doi.org/10.1016/S0167-2738(02)00362-4

[7] Duy, N.V., Jung, S.W., Nga, N.T., Son, D.N., Cho, J.H., Lee, S.H., Lee, W.B. and Yi, J.S. (2010) The Investigation of an Amorphous SiO_x System for Charge Storage Applications in Nonvolatile Memory at Low Temperature Process. *Materials Science and Engineering*: *B*, **175**, 176-180. http://dx.doi.org/10.1016/j.mseb.2010.07.009

[8] Pei, L.Z. (2008) Hydrothermal Deposition and Characterization of Silicon Oxide Nanospheres. *Materials Characterization*, **59**, 656-659. http://dx.doi.org/10.1016/j.matchar.2007.04.011

[9] Rao, K.S., Hami, K.E., Kodaki, T., Matsushige, K. and Makino, K. (2005) A Novel Method for Synthesis of Silica Nanoparticles. *Journal of Colloid and Interface Science*, **289**, 125-131. http://dx.doi.org/10.1016/j.jcis.2005.02.019

[10] Hong, Y.C. and Uhm, H.S. (2005) Production of Carbon Nanotubes by Microwave Plasma Torch at Atmospheric Pressure. *Physics of Plasma*, **12**, Article ID: 053504. http://dx.doi.org/10.1063/1.1914805

[11] Shin, D.H., Hong, Y.C. and Uhm, H.S. (2005) Production of Nanocrystalline Titanium Nitride Powder by Atmospheric Microwave Plasma Torch in Hydrogen/Nitrogen Gas. *Journal of the American Ceramic Society*, **88**, 2736-2739. http://dx.doi.org/10.1111/j.1551-2916.2005.00523.x

[12] Hong, Y.C., Bang, C.U., Shin, D.H. and Uhm, H.S. (2005) Band Gap Narrowing of TiO_2 by Nitrogen Dopingin Atmospheric Microwave Plasma. *Materials Chemistry and Physics*, **413**, 454-457. http://dx.doi.org/10.1016/j.cplett.2005.08.027

[13] Shin, D.H., Bang, C.U., Hong, Y.C. and Uhm, H.S. (2006) Preparation of Vanadium Pentoxide Powders by Microwave Plasma-Torch at Atmospheric Pressure. *Materials Chemistry and Physics*, **99**, 269-275. http://dx.doi.org/10.1016/j.matchemphys.2005.10.026

[14] Green, K. M., Borras, M. C., Woskov, P. P., Flores, G. J., Hadidi. K. and Thomas, P. (2002) Electronic Excitation Temperature Profiles in an Air Microwave Plasma Torch. *IEEE Transactions on Plasma Sciences*, **29**, 399.

[15] Kim, M.K., Jang, B.Y., Lee, J.S., Kim, J.S. and Nahm, S. (2013) Microstructures and Electrochemical Performances of Nano-Sized SiO_x ($1.18 \leq x \leq 1.83$) as an Anode Material for a Lithium(Li)-Ion Battery. *Journal of Power Sources*, **244**, 115-121. http://dx.doi.org/10.1016/j.jpowsour.2013.03.041

[16] Jun, Y.S., Jang, B.Y., Kim, J.S., Lee, J.S., Choi, C.H. and Han, M.H. (2013) Effects of Hydrogen Gas Injection on the Properties of SiO_x Nanoparticles Synthesized by Using an Evaporation and Condensation Process. *Journal of the Korean Physical Society*, **62**, 606-611. http://dx.doi.org/10.3938/jkps.62.606

[17] Sun, W., Qian, C., Cui, X.S., Wang, L., Wei, M., Casillas, G., Helmy, A.S. and Ozin, G.A. (2016) Silicon Monoxide—A Convenient Precursor for Large Scale Synthesis of near Infrared Emitting Monodisperse Silicon Nanocrystals. *Nanoscale*, **8**, 3678-3684. http://dx.doi.org/10.1039/C5NR09128D

[18] Doh, C.H., Shin, H.M., Kim, D.H., Ha, Y.C., Jin, B.S., Kim, H.S., Moon, S.I. and Veluchamy, A. (2008) Improved Anode Performance of Thermally Treated SiO/C Composite with an Organic Solution Mixture. *Electrochemistry Communications*, **10**, 233-237. http://dx.doi.org/10.1016/j.elecom.2007.11.034

[19] Veluchamy, A., Doh, C.H., Kim, D.H., Lee, J.H., Lee, D.J., Ha, K.H., Shin, H.M., Jin, B.S., Kim, H.S., Moon, S.I. and Park, C.W. (2009) Improvement of Cycle Behavior of SiO/C Anode Composite by Thermochemically Generated Li_4SiO_4 Inert Phase for Lithium Batteries. *Journal of Power Sources*, **188**, 574-577. http://dx.doi.org/10.1016/j.jpowsour.2008.11.137